

Gamma-ray bursts: Potential sources of ultra high energy cosmic-rays

E. Waxman^a *

^aPhysics Faculty, Weizmann Institute of Science, Rehovot 76100, Israel
waxman@wicc.weizmann.ac.il

The arguments suggesting an association between the sources of cosmological gamma-ray bursts (GRBs) and the sources of ultra-high energy cosmic rays (UHECRs) are presented. Recent GRB and UHECR observations are shown to strengthen these arguments. Predictions of the GRB model for UHECR production, that may be tested with large area high energy cosmic-ray detectors which are either operating or under construction, are outlined.

1. Introduction

The origin of UHECR's is one of the most exciting open questions of high energy astrophysics [1,2]. The extreme energy of the highest energy events poses a challenge to models of particle acceleration. Since very few known astrophysical objects have characteristics indicating that they may allow acceleration of particles to the observed high energies [3], the question of whether GRBs are possible UHECR sources is of great interest. Moreover, since the GRB model for UHECR production makes unique predictions, which differ from those of other models [4], the design and analysis of future UHECR experiments, as well as of high energy neutrino and photon experiments, may be affected by the answer to this question.

The phenomenology of GRBs, bursts of 0.1 MeV–1 MeV photons lasting for a few seconds [5], suggests that the observable effects are due to the dissipation of the kinetic energy of a cosmologically distant, relativistically expanding wind, a “fireball,” whose primal cause is not yet known [6,7,8]. Waxman [9], Milgrom & Usov [10] and Vietri [11] have independently suggested that ultra-high energy, $> 10^{19}$ eV, cosmic rays may be produced in GRB sources. The model suggested in ref. [9] was based on two arguments. First, it was shown that the constraints imposed on the

relativistic wind by the requirement that it produces observed GRB characteristics are similar to the constraints imposed on such a wind by the requirement that it would allow proton acceleration to $> 10^{20}$ eV. Second, the energy generation rate of γ -rays by GRBs was shown to be similar to the energy generation rate required to account for the observed UHECR flux [9,12].

In § 2 we briefly describe the model proposed in ref. [9] for UHECR production in GRB fireballs. In § 3 we discuss the implications of recent GRB and UHECR observations to this model (for a more detailed discussion, see [13]). In § 4 we discuss predictions of the model that may be tested with high energy cosmic-ray experiments. For predictions of the model that may be tested with high energy neutrino detectors see [4,14,15] and references therein. Our conclusions are discussed in § 5.

2. Production of UHECRs in GRBs

2.1. Proton acceleration

General phenomenological considerations, based on γ -ray observations, indicate that, regardless of the nature of the underlying sources, GRB's are produced by the dissipation of the kinetic energy of a relativistic expanding fireball. A compact source, $r_0 \sim 10^7$ cm, produces a wind, characterized by an average luminosity $L \sim 10^{52}$ erg s⁻¹ and mass loss rate \dot{M} . At small radius, the wind bulk Lorentz factor, Γ , grows linearly with radius, until most of the wind energy is converted to kinetic energy and Γ saturates at

*To appear in Nuclear Physics B (Proceedings Supplement), Proc. XIII International Symposium on Very High Energy Cosmic Ray Interactions (Pylos Greece, September 2004)

$\Gamma \sim L/\dot{M}c^2 \sim 300$. Variability of the source on a time scale $\Delta t \sim 10$ ms, resulting in fluctuations in the wind bulk Lorentz factor Γ on a similar time scale, results in internal shocks in the ejecta at a radius $r \sim r_d \approx \Gamma^2 c \Delta t \gg r_0$. It is assumed that internal shocks reconvert a substantial part of the kinetic energy to internal energy, which is then radiated as γ -rays by synchrotron and inverse-Compton radiation of shock-accelerated electrons. At a later stage, the shock wave driven into the surrounding medium by the expanding fireball ejecta leads to the emission of the lower-energy afterglow.

The observed radiation is produced, both during the GRB and the afterglow, by synchrotron emission of shock accelerated electrons. In the region where electrons are accelerated, protons are also expected to be shock accelerated. Thus, it is likely that protons, as well as electrons, are accelerated to high energy within GRB fireballs.

The internal shocks within the expanding wind are expected to be mildly relativistic in the wind rest frame, due to the fact that the allowed range of Lorentz factor fluctuations within the wind is from few $\times 10^2$ (the lower limit required to avoid large optical depth) to few $\times 10^3$ (the maximum Lorentz factor to which shell acceleration by radiation pressure is possible, e.g. [8]). This implies that the Lorentz factors associated with the relative velocities are not very large. Since internal shocks are mildly relativistic, we expect our understanding of non-relativistic shock acceleration to apply to the acceleration of protons in these shocks. In particular, the predicted energy distribution of accelerated protons is expected to be $dn_p/d\epsilon_p \propto \epsilon_p^{-2}$, similar to the electron energy spectrum inferred from the observed photon spectrum.

A power law energy spectrum with index 2 has been observed for non-relativistic shocks (see, e.g., ref. [16] and references therein) and for relativistic shocks [17]. It is consistent with that expected theoretically for Fermi acceleration in collisionless shocks [16,18], although a first principles understanding of the process is not yet available (see, e.g. ref. [19] for a discussion of alternative shock acceleration processes).

Several constraints must be satisfied by wind

parameters in order to allow proton acceleration to high energy ϵ_p . We summarize below these constraints. The reader is referred to refs. [9,4] for a detailed derivation. The requirement that the acceleration time, assumed to be comparable to the Larmor gyration time of the accelerated particle, be smaller than the wind expansion time, which also implies that the proton is confined to the acceleration region over the required time, sets a lower limit to the strength of the wind magnetic field. This may be expressed as a lower limit to the ratio of magnetic field to electron energy density [9],

$$u_B/u_e > 0.02\Gamma_{2.5}^2 \epsilon_{p,20}^2 L_{\gamma,52}^{-1}, \quad (1)$$

where $\epsilon_p = 10^{20} \epsilon_{p,20}$ eV, $\Gamma = 10^{2.5} \Gamma_{2.5}$ and $L_\gamma = 10^{52} L_{\gamma,52}$ erg/s is the wind γ -ray luminosity. A second constraint is imposed by the requirement that the proton acceleration time be smaller than the proton energy loss time, which is dominated by synchrotron emission. This sets an upper limit to the magnetic field strength, which in turn sets a lower limit to Γ [9,20]

$$\Gamma > 130 \epsilon_{p,20}^{3/4} \Delta t_{-2}^{-1/4}. \quad (2)$$

Here, $\Delta t = 10^{-2} \Delta t_{-2}$ s. As explained in [9], the constraints Eq. (1) and Eq. (2) hold regardless of whether the fireball is a sphere or a narrow jet (as long as the jet opening angle is $> 1/\Gamma$). The luminosity in Eq. 1 is the "isotropic equivalent luminosity", i.e. the luminosity under the assumption of isotropic emission.

Internal shocks within the wind take place at a radius $r_d \approx \Gamma^2 c \Delta t$. The constraint of Eq. (1) is independent of Δt , i.e. independent of the internal collision radius, while the constraint of Eq. (2) sets a lower limit to the collision radius for a given Δt . This implies that protons may be accelerated to $> 10^{20}$ eV regardless of the value of Δt , which may range from the dynamical time of the source ($\Delta t \sim 1$ ms) to the wind duration ($\Delta t \sim 1$ s), provided the magnetization and Lorentz factor are sufficiently large, following Eqs. 1 and 2.

At large radii the external medium affects fireball evolution, and a "reverse shock" is driven backward into the fireball ejecta and decelerates it. For typical GRB fireball parameters this shock

is also mildly relativistic (e.g. [8]), and its parameters are similar to those of an internal shock with $\Delta t \sim 10$ s. Protons may therefore be accelerated to $> 10^{20}$ eV not only in the internal wind shocks, but also in the reverse shock [21,4]. This implies that proton acceleration to $> 10^{20}$ eV is possible, provided the constraints of Eqs. 1 and 2 (with $\Delta t \sim 10$ s) are satisfied, also in (the currently less favorable) scenario where GRB γ -rays are produced in the shock driven by the fireball into the surrounding gas, rather than by internal collisions, as suggested, e.g., in [22].

The constraints given by Eqs. (1) and (2) are remarkably similar to those inferred from γ -ray observations, based on independent physical arguments: $\Gamma > 300$ is implied by the γ -ray spectrum by the requirement to avoid high pair-production optical depth, and magnetic field close to equipartition, $u_B/u_e \sim 0.1$, is required in order to account for the observed γ -ray emission [6,7,8]. This was the basis for the association of GRB's and UHECR's suggested in [9].

It should be noted here, that the only assumption related to the acceleration process made in the derivation of the constraints (1) and (2) is that the acceleration time is comparable to the Larmor gyration time of the accelerated particle. These constraints are valid therefore not only for Fermi-type shock acceleration, but rather to any electromagnetic acceleration process. This point is illustrated, for example, by the results of the analysis of ref. [23], where a non Fermi-type electromagnetic acceleration process is considered.

2.2. gamma-ray and UHECR energy production rates

The GRB model for UHECR production was suggested prior to the detection of GRB afterglows [24]. Estimates of the rate of GRBs were based at that time on the γ -ray flux distribution, and ranged from $\sim 3/\text{Gpc}^3\text{yr}$ [25] to $\sim 30/\text{Gpc}^3\text{yr}$ [26]. The estimated average γ -ray energy release in a single GRB, based on a characteristic peak flux of $\sim 10^{51}\text{erg/s}$ [5], was $\sim 10^{52}$ erg. These estimates were subject to large uncertainties, since the γ -ray luminosity function as well as the evolution of GRB rate with redshift were poorly constrained. Based on the rate and energy estimates,

the rate of γ -ray energy generation by GRBs was estimated to be $\sim 10^{44}\text{erg}/\text{Mpc}^3\text{yr}$. This rate is similar to the energy generation rate in cosmic-rays of energy in the range of 10^{19} eV to 10^{21} eV, $4.5 \pm 1.5 \times 10^{44}\text{erg}/\text{Mpc}^3\text{yr}$, inferred from Fly's Eye and AGASA measurements of the UHECR flux available at the time the GRB model for UHECR production was proposed [12].

The determination of GRB redshifts, which was made possible by the detection of afterglows, allows a more reliable estimate of the GRB energy production rate, and the increased exposure of UHECR experiments, provided by AGASA and HiRes, allows a more accurate estimate of the UHECR energy production rate. The implications of these more recent observations is discussed in § 3.2.

3. Implications of recent GRB and UHECR observations

3.1. Proton acceleration

Afterglow observations [24] lead to the confirmation of the cosmological origin of GRBs and confirmed standard model predictions of afterglow that results from synchrotron emission of electrons accelerated to high energy in the highly relativistic shock driven by the fireball into its surrounding gas [6,7,8]. Afterglow observations provide therefore strong support for the underlying fireball scenario. In addition, afterglow observations provide important information on the values of model parameters that enter the constraints given by Eqs. (1) and (2).

Prior to the detection of afterglows, it was commonly assumed that the farthest observed GRB's lie at redshift $z \sim 1$ [26,25]. Based on afterglow redshift determinations, we now know that detected GRB's typically lie at farther distances (e.g. [27]). This implies that the characteristic GRB luminosity is higher by an order of magnitude compared to pre-afterglow estimates, $L_\gamma \approx 10^{52}\text{erg/s}$ instead of $L_\gamma \approx 10^{51}\text{erg/s}$. This relaxes the constraint on magnetic field energy fraction given by Eq. (1).

In several cases, fast follow up afterglow observations allowed the detection of radio and optical emission from the reverse shock (e.g. [28,29]).

These observations provide direct information on the plasma conditions in the reverse shock, where acceleration of protons to high energy may take place. Two major conclusions were drawn from the analysis of the early optical and radio reverse shock emission. First, lower limits to the initial fireball Lorentz factors were inferred, in the range of $\Gamma > 100$ to $\Gamma > 1000$ [28,29]. Second, the magnetic field in the reverse shock was inferred to be close to equipartition, that is u_B/u_e was inferred to be of order unity [30,28]. Early afterglow observations provide therefore constraints on Γ and on u_B/u_e which are (i) Independent of the constraints derived from γ -ray observations; (ii) Consistent with the γ -ray constraints; and (iii) Are remarkably similar to the constraints of Eqs. (1) and (2), that need to be satisfied in order to allow proton acceleration to $> 10^{20}$ eV.

3.2. gamma-ray and UHECR energy production rates

3.2.1. gamma-ray production rate

Most of the GRBs are observed from $z > 1$, since they can be detected out to large redshift. This implies that the GRB rate density at $z > 1$ is better constrained by the observations than the local, $z = 0$, rate. The inferred local rate depends on the assumed redshift evolution. It is now commonly believed that the GRB rate evolves with redshift following the star-formation rate, based on the association of GRBs with type Ib/c supernovae. This association is based on the temporal and angular coincidence of several GRBs and type Ib/c supernovae [31,32,33], and on evidence for optical supernovae emission in several GRB afterglows [34]. Adopting the assumption, that the GRB rate follows the redshift evolution of the star formation rate, the local ($z = 0$) GRB rate density is [35] $R_{\text{GRB}}(z = 0) \approx 0.5 \times 10^{-9} \text{Mpc}^{-3} \text{yr}^{-1}$. Given the current (systematic uncertainties in the redshift) data, this rate is accurate to within a factor of a few [35].

The local energy generation rate in γ -rays by GRB's, $\dot{\epsilon}_\gamma$, is given by the product of $R_{\text{GRB}}(z = 0)$ and the average γ -ray energy release in a single GRB, ϵ_γ . [27] provide ϵ_γ for 27 bursts with known redshifts, in a standard rest-frame bandpass, 0.02 MeV to 2 MeV. The average is

$\epsilon_\gamma = 2.9 \times 10^{53}$ erg, with estimated uncertainty, due to the correction to a fixed rest-frame bandpass, of $\sim 20\%$ for individual bursts (and much smaller for the average). In calculating $\dot{\epsilon}_\gamma$ from this value of ϵ_γ , the following point should be taken into account. ϵ_γ is the average energy for bursts with known redshift, most of which were localized by the BeppoSAX satellite. Since BeppoSAX has a higher detection flux threshold than BATSE [36,35], it is sensitive to $\approx 70\%$ of the bursts detectable by BATSE, for which the GRB rate $R_{\text{GRB}}(z = 0)$ was inferred. Thus, the energy generation rate by bursts detectable by BeppoSAX is

$$\begin{aligned} \dot{\epsilon}_\gamma^{\text{GRB}}[0.02\text{MeV}, 2\text{MeV}] &\approx 0.7 R_{\text{GRB}}(z = 0) \epsilon_\gamma \\ &= 10^{44} \text{erg Mpc}^{-3} \text{yr}^{-1}. \end{aligned} \quad (3)$$

The energy observed in γ -rays in the range of BATSE is dominated by photons in the energy range of 0.1 MeV to 1 MeV, and therefore reflects the energy of accelerated electrons over roughly half a decade of electron energies (recall that for synchrotron and inverse-Compton emission the photon energy is proportional to the square of the electron energy). Thus, the rate of energy generation per logarithmic interval of electron energy is

$$\begin{aligned} \epsilon_e^2 \frac{dn_e^{\text{GRB}}}{d\epsilon_e} &\approx \dot{\epsilon}_\gamma^{\text{GRB}}[0.02\text{MeV}, 2\text{MeV}] \\ &\approx 10^{44} \text{erg Mpc}^{-3} \text{yr}^{-1}. \end{aligned} \quad (4)$$

The main uncertainty in determining $\dot{\epsilon}_\gamma$ is related to the uncertainty in the local GRB rate, due to which the value given in Eq. 3 is accurate to within a factor of few. It should be noted that the numbers quoted above for the GRB rate density and γ -ray energy release are based on the assumption that GRB γ -ray emission is isotropic. If, as now commonly believed, the emission is confined to a solid angle $\Delta\Omega < 4\pi$, then the GRB rate is increased by a factor $(\Delta\Omega/4\pi)^{-1}$ and the GRB energy is decreased by the same factor. However, their product, the energy generation rate, is independent of the solid angle of emission.

3.2.2. UHECR production rate

The cosmic-ray spectrum flattens at $\sim 10^{19}$ eV [37,38]. There are indications that the spectral change is correlated with a change in composition, from heavy to light nuclei [37,39,40] (see, however, [41]). These characteristics suggest that the cosmic ray flux is dominated at energies $< 10^{19}$ eV by a Galactic component of heavy nuclei, and at UHE by an extra-Galactic source of protons. Also, both the AGASA and Fly's Eye experiments report an enhancement of the cosmic-ray flux near the Galactic disk at energies $\leq 10^{18.5}$ eV, but not at higher energies [42,43]. Fly's Eye stereo spectrum is well fitted in the energy range $10^{17.6}$ eV to $10^{19.6}$ eV by a sum of two power laws: A steeper component, with differential number spectrum $J \propto \epsilon^{-3.50}$, dominating at lower energy, and a shallower component, $J \propto \epsilon^{-2.61}$, dominating at higher energy, $\epsilon > 10^{19}$ eV. The data are consistent with the steeper component being composed of heavy nuclei primaries, and the lighter one being composed of proton primaries.

The observed UHECR flux and spectrum may be accounted for by a two component model [44], with a Galactic component given by the Fly's Eye fit, $\frac{dn}{d\epsilon} \propto \epsilon^{-3.50}$, and an extra-Galactic component characterized by a local ($z = 0$) energy generation rate of extra-Galactic protons of

$$\epsilon_p^2 \frac{dn_p^{\text{CR}}}{d\epsilon_p} = 0.65 \times 10^{44} \text{erg Mpc}^{-3} \text{yr}^{-1}. \quad (5)$$

Uncertainties in the absolute energy calibration of the experiments lead to uncertainty of $\approx 20\%$ in this rate [44]. The spectral index, 2, is that expected for acceleration in sub-relativistic collisionless shocks in general, and in particular for the GRB model discussed in § 2.1. The model used in [44] is similar to that proposed in [12]. The improved constraints on UHECR spectrum and flux provided by the recent observations of HiRes do not change the estimates given in [12] for the energy generation rate and spectrum, Eq. (5), but reduce the uncertainties.

Comparing eqs. (5) and (3) we find that the observed UHECR flux and spectrum may be accounted for if GRBs produce high energy electrons and protons with similar spectra and rates.

It should be emphasized here, that the ratio between the energy carried by relativistic electrons and protons in collisionless shocks is not known from basic principles. Moreover, as explained above, the estimate of the GRB gamma-ray energy generation rate is uncertain by a factor of a few. Thus, an exact match between the derived γ -ray and UHECR generation rates should not necessarily be expected. Given current uncertainties, the two rates should only be expected to be of the same order of magnitude.

Finally, the following point should be mentioned. We have so far discussed the contribution of extra-Galactic GRBs to the UHECR flux. GRBs exploding within our Galaxy may also contribute to the Galactic cosmic-ray flux at lower energies, $> 10^{15}$ eV [45]. However, in order for GRBs to make a significant contribution to the flux at $\sim 10^{15}$ eV, they should produce more energy in $\sim 10^{15}$ eV protons than they are inferred (based on their gamma-ray emission) to produce in high energy electrons [46].

4. Predictions for high energy cosmic-ray experiments

The initial proton energy, necessary to have an observed energy ϵ_p , increases with source distance due to propagation energy losses. The rapid increase of the initial energy after it exceeds, due to electron-positron production, the threshold for pion production effectively introduces a cutoff distance, $D_c(\epsilon_p)$, beyond which sources do not contribute to the flux above ϵ_p . The function $D_c(\epsilon_p)$ is shown in Fig. 1 (adapted from [47]). Since $D_c(\epsilon_p)$ is a decreasing function of ϵ_p , for a given number density of sources there is a critical energy ϵ_c , above which only one source (on average) contributes to the flux. In the GRB model ϵ_c depends on the product of the burst rate R_{GRB} and the time delay. The number of sources contributing, on average, to the flux at energy ϵ_p is [47]

$$N(\epsilon_p) = \frac{4\pi}{5} R_{GRB} D_c(\epsilon_p)^3 \tau[\epsilon_p, D_c(\epsilon_p)] \quad , \quad (6)$$

where $\tau(\epsilon_p, D)$, the spread in arrival time of protons of energy ϵ_p produced by a source at dis-

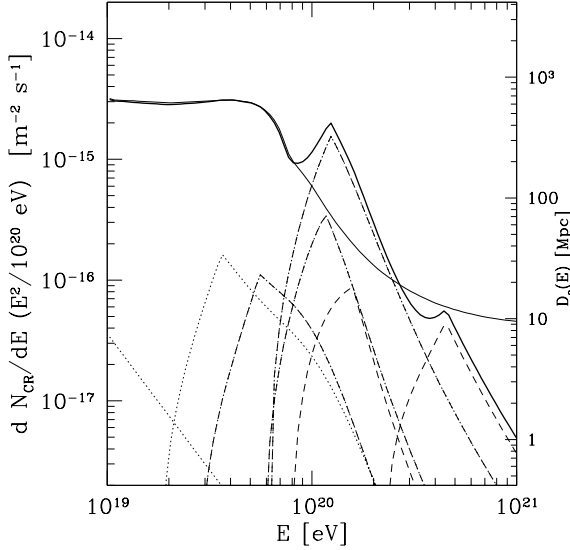


Figure 1. Results of a Monte-Carlo realization of the bursting sources model, with $\epsilon_c = 1.4 \times 10^{20}$ eV: Thick solid line- overall spectrum in the realization; Thin solid line- average spectrum, this curve also gives $D_c(\epsilon_p)$; Dotted lines- spectra of brightest sources at different energies.

tance D due to deflection by inter-galactic magnetic fields, is [9,47]

$$\tau(\epsilon_p, D) \approx 10^7 \epsilon_{p,20}^{-2} D_{100}^2 \lambda_{\text{Mpc}} B_{-8}^2 \text{ yr}. \quad (7)$$

Here $D = 100 D_{100} \text{ Mpc}$, $\lambda = 1 \lambda_{\text{Mpc}} \text{ Mpc}$ is the characteristic length scale over which the field direction varies, and $B = 10^{-8} B_{-8} \text{ G}$ is the characteristic field amplitude. The average intensity resulting from all sources is

$$J(\epsilon_p) = \frac{1}{4\pi} R_{GRB} \frac{dn_p}{d\epsilon_p} D_c(\epsilon_p) \quad , \quad (8)$$

where $dn_p/d\epsilon_p$ is the number per unit energy of protons produced on average by a single burst (this is the formal definition of $D_c(\epsilon_p)$).

The critical energy ϵ_c , beyond which a single source contributes on average to the flux,

$$\frac{4\pi}{5} R_{GRB} D_c(\epsilon_c)^3 \tau[\epsilon_c, D_c(\epsilon_c)] = 1 \quad , \quad (9)$$

depends on the unknown properties of the intergalactic magnetic field, $\tau \propto B^2 \lambda$. However, the rapid decrease of $D_c(\epsilon_p)$ with energy near 10^{20} eV implies that ϵ_c is only weakly dependent on the value of $B^2 \lambda$. In The GRB model, the product $R_{GRB} \tau (D = 100 \text{ Mpc}, \epsilon_p = 10^{20} \text{ eV})$ is approximately limited to the range 10^{-6} Mpc^{-3} to 10^{-2} Mpc^{-3} (The lower limit is set by the requirement that at least a few GRB sources be present at $D < 100 \text{ Mpc}$, and the upper limit by the Faraday rotation bound $B \lambda^{1/2} \leq 10^{-8} \text{ G Mpc}^{1/2}$ [48], and $R_{GRB} \leq 1/\text{Gpc}^3 \text{ yr}$). The corresponding range of values of ϵ_c is $10^{20} \text{ eV} \leq \epsilon_c < 4 \times 10^{20} \text{ eV}$.

Fig. 1 presents the flux obtained in one realization of a Monte-Carlo simulation described by Miralda-Escudé & Waxman [47] of the total number of UHECRs received from GRBs at some fixed time. For each realization the positions (distances from Earth) and times at which cosmological GRBs occurred were randomly drawn, assuming an intrinsic proton generation spectrum $dn_p/d\epsilon_p \propto \epsilon_p^{-2}$, and $\epsilon_c = 1.4 \times 10^{20}$ eV. Most of the realizations gave an overall spectrum similar to that obtained in the realization of Fig. 1 when the brightest source of this realization (dominating at 10^{20} eV) is not included. At $\epsilon_p < \epsilon_c$, the number of sources contributing to the flux is very large, and the overall UHECR flux received at any given time is near the average (the average flux is that obtained when the UHECR emissivity is spatially uniform and time independent). At $\epsilon_p > \epsilon_c$, the flux will generally be much lower than the average, because there will be no burst within a distance $D_c(\epsilon_p)$ having taken place sufficiently recently. There is, however, a significant probability to observe one source with a flux higher than the average. A source similar to the brightest one in Fig. 1 appears $\sim 5\%$ of the time.

At any fixed time a given burst is observed in UHECRs only over a narrow range of energy, because if a burst is currently observed at some energy ϵ_p then UHECRs of much lower energy from this burst have not yet arrived, while higher energy UHECRs reached us mostly in the past. As mentioned above, for energies above the pion production threshold, $\epsilon_p \sim 5 \times 10^{19}$ eV, the dispersion in arrival times of UHECRs with fixed

observed energy is comparable to the average delay at that energy. This implies that the spectral width $\Delta\epsilon_p$ of the source at a given time is of order the average observed energy, $\Delta\epsilon_p \sim \epsilon_p$. Thus, bursting UHECR sources should have narrowly peaked energy spectra, and the brightest sources should be different at different energies. For steady state sources, on the other hand, the brightest source at high energies should also be the brightest one at low energies, its fractional contribution to the overall flux decreasing to low energy only as $D_c(\epsilon_p)^{-1}$. A detailed numerical analysis of the time dependent energy spectrum of bursting sources is given in [49,50].

5. Conclusions

The main constraints that a relativistic wind (fireball) need to satisfy to allow proton acceleration to $> 10^{20}$ eV are given by Eqs. (1) and (2): The magnetic field energy density u_B should exceed a few percent of the relativistic electron energy density u_e , and the wind Lorentz factor Γ should exceed $\approx 10^2$. As explained in § 2.1, these constraints are independent of the details of the acceleration process, and are valid for any electromagnetic acceleration process. The similarity of these constraints and the constraints imposed on wind parameters, based on independent physical considerations, by γ -ray observations were the basis for the association of GRB and UHECR sources suggested in [9]. We have pointed out in § 3.1 that afterglow observations of GRBs imply a higher characteristic GRB luminosity than estimated based on γ -ray observations alone, thus relaxing the constraint of Eq. (1) on u_B/u_e . Moreover, early optical and radio afterglow observations provide new constraints on wind parameters, implying large Lorentz factors, $\Gamma > 10^2$ to $\Gamma > 10^3$, and large magnetic field energy density in the fireball plasma, $u_B/u_e \sim 1$. These constraints are consistent with those previously inferred from γ -ray observations, and with the constraints imposed by the requirement to allow proton acceleration to $> 10^{20}$ eV.

We have also pointed out, in § 2.2, that GRBs produce high energy electrons at a rate (and with a spectrum) similar to the rate (and spectrum) at

which high energy protons should be produced in order to account for the UHECR spectrum and flux. Thus, the observed UHECR flux and spectrum may be accounted for if GRBs produce high energy electrons and protons at a similar rate and spectrum.

In § 4 we have pointed out that the local GRB rate implies that the rate of GRBs out to a distance from which most protons of energy exceeding 10^{20} eV originate, $\simeq 90$ Mpc (see fig. 1), is $\sim 10^{-3}/\text{yr}$. The number of GRBs contributing to the observed flux at any given time, eq. (6) is given by the product of this rate and the spread in arrival time of protons, due to the combined effect of stochastic propagation energy loss and deflection by magnetic fields. This time spread, eq. (7), may be as large as 10^7 yr for 10^{20} eV originating at 90 Mpc distance, implying that the number of GRBs contributing to the $> 10^{20}$ eV flux at any given time may reach $\sim 10^4$. The upper limit on the strength of the inter-galactic magnetic field, combined with the low local rate of GRB's, leads to unique predictions of the GRB model for UHECR production [47,51], that may be tested with operating [52], under-construction [53] and planned [54] large area UHECR detectors. In particular, a critical energy is predicted to exist, $10^{20}\text{eV} \leq E_c < 4 \times 10^{20}\text{eV}$, above which a few sources produce most of the UHECR flux, and the observed spectra of these sources is predicted to be narrow, $\Delta\epsilon/\epsilon \sim 1$: The bright sources at high energy should be absent in UHECRs of much lower energy, since particles take longer to arrive the lower their energy.

Acknowledgments.

This research was partially supported by MINERVA and AEC grants.

REFERENCES

1. Bhattacharjee, P. & Sigl, G. 2000, Phys. Rep. 327, 109.
2. Nagano, M. & Watson, A. A. 2000, Rev. Mod. Phys. 72, 689.
3. Waxman, E. 2004, Pramana 62, 483 (Proc. PASCOS 03, Mumbai India; astro-ph/0310079).

4. Waxman, E. 2001, Lect. Notes Phys. **576**, 122-154 (astro-ph/0103186).
5. Fishman, G. J. & Meegan, C. A. 1995, ARA&A **33**, 415.
6. Piran, T. 2000, Phys. Rep. **333**, 529.
7. Mészáros, P. 2002, ARA&A **40**, 137
8. Waxman, E. 2003, Lect. Notes Phys. **598**, 393 (astro-ph/0303517).
9. Waxman, E. 1995, Phys. Rev. Lett. **75**, 386.
10. Milgrom, M. & Usov, V. 1995, Ap. J. **449**, L37.
11. Vietri, M. 1995, Ap. J. **453**, 883.
12. Waxman, E. 1995, Astrophys. J. Lett. **452**, L1.
13. Waxman, E. 2004, Astrophys. J. **606**, 988.
14. Mészáros, P. et al. 2003, AIP Conference Proceedings, Vol. 727, 125.
15. Halzen, F. 2004, Nucl. Phys. **B136**, 93.
16. Blandford, R. & Eichler, D. 1987, Phys. Rep. **154**, 1.
17. Waxman, E. 1997, Astrophys. J. **485**, L5; Freedman, D. L. & Waxman, E. 2001, Astrophys. J. **547**, 922; Berger, I., Kulkarni, S. R. & Frail, D. A. 2003 Astrophys. J. **590**, 379.
18. Bednarz, J. & Ostrowski, M. 1998, Phys. Rev. Lett. **80**, 3911; Kirk, J. K. et al. 2000, Phys. Rev. **542**, 235; Keshet, U. & Waxman, E. 2004, to appear in Phys.Rev.Lett. (astro-ph/0408489).
19. Arons, J. & Tavani, M. 1994, Astrophys. J. Supp. **90**, 797.
20. Rachen, J. P., & Mészáros, P. 1998, Phys. Rev. D **58**, 123005.
21. Waxman, E., & Bahcall, J. N. 2000, Ap. J. **541**, 707.
22. Dermer, C. D. 1999, A&AS **138**, 519.
23. Gialis, D. & Pelletier, G. 2004. A&A **425**, 395; Gialis, D. & Pelletier, G., submitted to Ap. J. (astro-ph/0405547).
24. Kulkarni, S. R. *et al.* 2000, Proc. of the 5th Huntsville Gamma-Ray Burst Symposium (astro-ph/0002168).
25. Piran, T. 1992, Ap. J. **389**, L45.
26. Mao, S. & Paczyński, B. 1992, Ap. J. **388**, L45.
27. Bloom, J., Frail, D. A. & Kulkarni, S.R., 2003, ApJ **594**, 674.
28. Zhang, B., Kobayashi, S. & Mészáros, P. 2003, ApJ **595**, 950.
29. Soderberg, A. M. & Ramirez-Ruiz, E. 2003, MNRAS **345**, 854.
30. Waxman, E. & Draine, B. T. 2000, Ap. J. **537**, 796.
31. Galama, T. J. 1998b, Nature **395**, 670
32. Stanek, K. Z. et al. 2003, Ap. J. **591**, L17
33. Hjorth, J. et al. 2003, Nature **423**, 847
34. Bloom, J. S. 2003, Proc. "Gamma Ray Bursts in the Afterglow Era, Third Workshop" (Rome, Sept 2002); astro-ph/0303478.
35. Guetta, D., Piran, T. & Waxman, E. 2003, to appear in ApJ (astro-ph/0311488).
36. Band, D. L. 2003, Ap. J. **588**, 945.
37. Bird, D. J. *et al.* 1994, Astrophys. J. **424**, 491.
38. Hayashida N. *et al.* 1999, Astrophys. J. **522**, 225 and astro-ph/0008102.
39. Dawson, B. R., Meyhandan, R., and Simpson, K. M., 1998, Astropart. Phys. **9**, 331.
40. Abu-Zayyad, T. et al. 2001, ApJ **557**, 686.
41. Watson, A. A. Proc. XIII ISVHECRI: Pylos, Greece (astro-ph/0410514).
42. Bird, D. J. *et al.* 1998, Astrophys. J. **511**, 739.
43. Hayashida N. *et al.* 1999a, Astropart. Phys. **10**, 303.
44. Bahcall, J. N. & Waxman, E. 2003, Phys. Lett. **B556**, 1
45. Milgrom, M. & Usov, V. 1996, Astropart. Phys. **4**, 365.
46. Wick, S. D., Dermer, C. D. & Atoyan, A. 2004 Astropart. Phys. **21**, 125.
47. Miralda-Escudé, J. & Waxman, E. 1996, Ap. J. **462**, L59.
48. Kronberg, P. P. 1994, Rep. Prog. Phys. **57**, 325.
49. Sigl, G., Lemoine, M. & Olinto, A. V. 1997, Phys. Rev. **D56**, 4470.
50. Lemoine, M., Sigl, G., Olinto, A. V. & Schramm, D. N. 1997, Ap. J. **486**, L115.
51. Waxman, E. & Miralda-Escudé, J. 1996, Ap. J. **472**, L89.
52. Abu-Zayyad, T., et al., 2004, Phys. Rev. Lett. **92**, 151101.
53. Cronin, J.W. 1992, Nucl. Phys. B (Proc. Suppl.) **28**, 313.
54. Teshima, M. et al. 1992, Nucl. Phys. B (Proc. Suppl.) **28**, 169.